Measurement of the $B^0 \to D^{*-}\pi^+\pi^-\pi^+$ branching fraction by BABAR

Alberto Lusiani[*]

Author Scuola Normale Superiore and INFN, sezione di Pisa

E-mail: alberto.lusiani@pi.infn.it

The BABAR collaboration measured the decay branching fraction $\mathscr{B}(\mathscr{B}' \to \mathscr{D}^{*-}\pi^+\pi^-\pi^+) = (\iota \in \neq \iota.\infty\infty\,(\text{stat.}) \pm \iota.\ni\infty\,(\text{syst.})) \times \infty\iota^{-\ni}$ using a sample of $(470.9 \pm 2.8) \times 10^6\ B\bar{B}$ pairs. This measurement will facilitate the measurement of $\mathscr{B}(\mathscr{B}' \to \mathscr{D}^{*-}\tau^+\nu_\tau)$ with $\tau^+ \to \pi^+\pi^-\pi^+\bar{\nu}_\tau$ at hadronic colliders, improving the experimental precision on the normalization branching fraction $\mathscr{B}(\mathscr{B}' \to \mathscr{D}^{*-}\pi^+\pi^-\pi^+)$.

38th International Conference on High Energy Physics
3-10 August 2016
Chicago, USA

---

[*]Speaker.

1. Introduction

Past measurements of $B \to D^{(*)}\tau\nu_\tau$ by BABAR [1] in 2012 and later by Belle [2, 3] and the LHCb measurement of $B \to D^*\tau\nu_\tau$ [4] have been combined by HFAG with measurements of $B \to D^{(*)}\ell\nu_\tau$ ($\ell = e, \mu$) to determine the ratios $R(X) \equiv \mathscr{B}(\mathscr{B} \to \mathscr{X}\,\tau\nu_\tau)/\mathscr{B}(\mathscr{B} \to \mathscr{X}\,\ell\nu_\ell)$. The resulting values $R(D)_{\text{exp}} = 0.397 \pm 0.040 \pm 0.028$ and $R(D^*)_{\text{exp}} = 0.316 \pm 0.016 \pm 0.010$ exceed the Standard Model (SM) predictions [5] $R_{\text{SM}}(D) = 0.297 \pm 0.017$ and $R_{\text{SM}}(D^*) = 0.252 \pm 0.003$ with a combined discrepancy of 4.0σ [6]. The measurement of $B \to D^*\tau\nu_\tau$ can be improved by combining a high precision measurement of the ratio $\mathscr{B}(\mathscr{B}' \to \mathscr{D}^{*-}\tau^+(\pi^+\pi^-\pi^+\overline{\nu}_\tau)\nu_\tau)/\mathscr{B}(\mathscr{B}' \to \mathscr{D}^{*-}\pi^+\pi^-\pi^+)$, which can be accomplished by LHCb, with an improved measurement of $\mathscr{B}(\mathscr{B}' \to \mathscr{D}^{*-}\pi^+\pi^-\pi^+)$, which can be done at the B-factories. With that motivation, BABAR has published the latter measurement, which is described in the following.

2. Data sample and selection

The analysis relies on a sample corresponding to $(470.9 \pm 2.8) \times 10^6$ $B\bar{B}$ pairs and an integrated luminosity of 424.2 ± 1.8 fb^{-1} collected at the $\Upsilon(4S)$ resonance.

Monte Carlo (MC) simulations are used to study background processes and signal reconstruction efficiencies. The EvtGen event generator [7] is used to simulate particle decays. The simulated events include samples of $e^+e^- \to q\bar{q}(\gamma)$ processes, where q is a u, d, s, or c quark and correspond to an equivalent luminosity of $2,589$ fb^{-1} and to $1,427 \times 10^6$ $B\bar{B}$ pairs. The detector response is simulated with Geant4 [8].

The $B^0 \to D^{*-}\ \pi^+\ \pi^-\ \pi^+$ decay chain is fully reconstructed. The D^{*-} mesons are reconstructed from $D^{*-} \to \bar{D}^0\pi^-$ candidates, the $\bar{D}^0$ mesons as $\bar{D}^0 \to K^+\pi^-$ candidates. Kaons are identified using information from the tracking and Cherenkov detectors. The $\bar{D}^0$ mass must lie within ± 20 MeV/c^2 (3 standard deviations) of the nominal $\bar{D}^0$ mass [9]. The slow pion combined with the $\bar{D}^0$ must have a momentum smaller than 0.45 GeV/c. The difference between the reconstructed mass of the D^{*-} candidate and the reconstructed mass of the $\bar{D}^0$ candidate must lie between 0.1435 and 0.1475 GeV/c^2. The B^0 candidate is obtained combining a D^{*-} candidate with three other charged-particle tracks. No pion particle identification is required. All other tracks belong to the "rest of the event" (ROE). Background coming from non-$B\bar{B}$ events is suppressed using a neural-network classifier using nine variables, computed the center-of-mass (CM) frame:

- the cosine of the angle between the B^0 candidate's thrust axis and the beam axis;

- the sphericity of the B^0 candidate;

- the thrust of the ROE;

- the sum over the ROE of p, where p is the magnitude of a particle's momentum;

- the sum over the ROE of $\frac{1}{2}(3\cos^2\theta - 1)p$, where θ is the polar angle of a particle's momentum;

- the cosine of the angle between the thrust axis of the B^0 candidate and the thrust axis of the ROE;

- the cosine of the angle between the sphericity axis of the B^0 candidate and the thrust axis of the ROE;

- the ratio of the second-order to zeroth-order Fox-Wolfram moment using all reconstructed particles [10];

- the cosine of the angle between the thrust axis calculated using all reconstructed particles and the beam axis.

A fraction of 69% of the non-$B\bar{B}$ events is suppressed, while keeping 80% of correctly reconstructed B^0 candidates. The B^0 candidate is required to have a CM energy ± 90 MeV (4 standard deviations) of $\sqrt{s}/2$ (the invariant mass of the initial state, determined by the beam energies). Multiple B^0 candidates in the same event are accepted without corrections, since the event candidate multiplicity is consistent between data and simulation. In the simulation, the signal and background events with at least one candidate have on average 1.57 and 1.37 B^0 candidates per event, respectively.

3. Signal and background yields

Figure 1 shows the energy-substituted mass $m_{ES} = \sqrt{s/4 - p_B^2}$ distribution for the selected data and for MC-simulated events. The m_{ES} distribution of correctly reconstructed signal candidates peaks near the B^0 mass. Signal and backgrounds yields are fit on this distribution. The signal
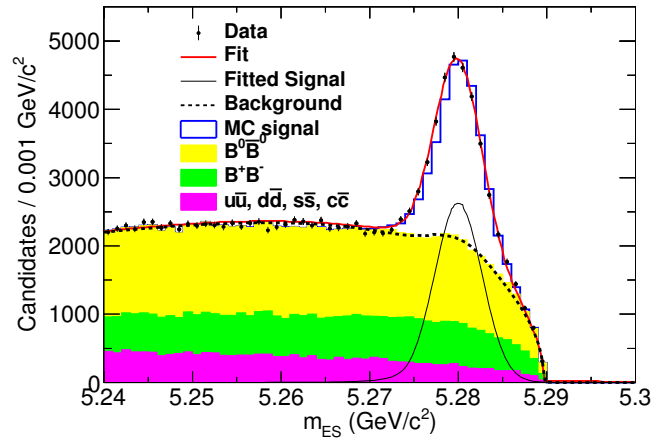

Figure 1: The m_{ES} distribution of B^0 candidates for data (points), MC simulations (histograms), and the unbinned extended-maximum-likelihood fit to the data (curves). The MC distributions are shown as stacked histograms. The $B^0 \to D^{*-}D_s^+$ with $D_s^+ \to \pi^+\pi^-\pi^+$ decays are part of the MC signal. The MC signal contribution is normalized such that its stacked histogram has the same integral as the data.

candidates m_{ES} distribution is modeled using a Crystal Ball [11, 12, 13] probability density function (PDF), with cutoff and power-law parameters determined from simulation. The background is modeled as sum of one non-peaking component from $e^+e^- \to q\bar{q}(\gamma)$ events, and two peaking components from B^+B^- and $B^0\bar{B}^0$ decays, respectively. The non-peaking component is modeled using an ARGUS function [14]. The two peaking components are modeled with Gaussian distributions

with mean, width and normalization fit on the respective simulated samples. A one-dimensional unbinned extended-maximum-likelihood fit on the m_{ES} distribution is performed with free parameters for the signal yield, the non-peaking background yield, the mean and width parameters of the Crystal Ball function, and the curvature parameter of the ARGUS function. The cutoff parameter for the ARGUS function is fixed to $\sqrt{s}/2$. The peaking background distributions are kept fixed to their simulation estimates and consist of 590 ± 120 and 1450 ± 130 candidates from B^+B^- and $B^0\bar{B}^0$ decays, respectively. The fit is shown in Fig. 1 and results in a signal yield of 17800 ± 300.

4. Study of the three-pion invariant mass distribution

The signal 3π mass distribution in Fig. 2 is obtained using all the events in the signal region, defined to be $5.273 < m_{ES} < 5.285$ GeV/c^2, and subtracting the events in the sideband region, corresponding to $5.240 < m_{ES} < 5.270$ GeV/c^2. The number of sideband events is rescaled to the total amount of background that is fit inside the signal region.
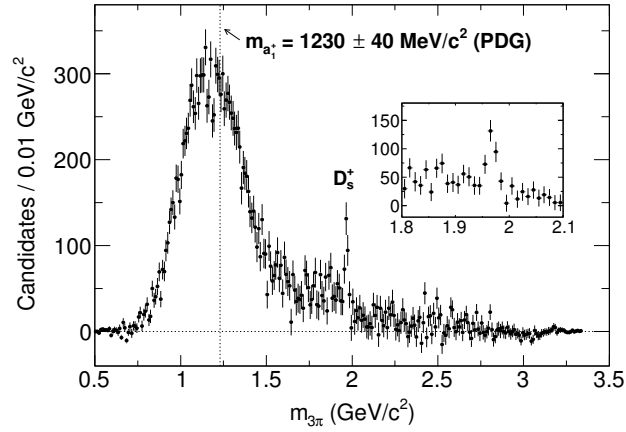

Figure 2: The background-subtracted invariant-mass spectrum of the 3π system. The inset shows the distribution around the D_s^+ region.

The distribution shows a peak at the D_s mass that corresponds to the decay chain $B^0 \to D^{*-}D_s^+(\pi^+\pi^-\pi^+)$. That contribution is removed from the signal yield by subtracting the events in the 1.9–2.0 GeV/c^2 region of the 3π invariant-mass distribution that exceed the interpolation of the bin contents in the 1.8–1.9 GeV/c^2 and 2.0–2.1 GeV/c^2 regions. The removed D_s^+ contribution consists of 233 ± 63 events on top of 326 ± 35 remaining signal events.

The 3π invariant mass of the signal Monte Carlo simulation is weigthed to reproduce the distribution observed in the data in order to get the signal efficiency.

5. Branching fraction measurement

The branching fraction is determined by dividing the signal yield by the signal efficiency (inclusive of the D^{*-} and $\bar{D}^0$ branching fractions that correspond to the event selection) and by the estimated number of B^0 mesons in the analyzed sample. Table 1 summarizes the systematic

Table 1: Summary of systematic uncertainties. The uncertainties are assumed to be uncorrelated, and so are added in quadrature.

Source	Uncertainty (%)
Fit algorithm and peaking backgrounds	2.4
Track-finding	2.0
$\pi^+\pi^-\pi^+$ invariant-mass modeling	1.7
D^{*-} and $\bar{D}^0$ decay branching fractions	1.3
$\Upsilon(4S) \to B^0\bar{B}^0$ decay branching fraction	1.2
K^+ identification	1.1
Signal efficiency MC statistics	0.9
Sideband subtraction	0.7
$B\bar{B}$ counting	0.6
Total	4.3

uncertainties. Uncertainties on the fit algorithm and the peaking background are estimated by accounting for the uncertainties on the fixed fit parameters, whose values are obtained from simulated events. The systematic uncertainty from tracking comes from studies on data samples by the BABAR collaboration. The uncertainty related to the reweighting of the 3π distribution is set to the full shift on the signal efficiency between before and after reweighting. Uncertainties on D^{*-}, $\bar{D}^0$ and $\Upsilon(4S) \to B^0\bar{B}^0$ branching fractions are taken from the world averages [9]. The kaon identification uncertainty is taken from studies on data samples by the BABAR collaboration. The signal efficiency uncertainty includes a contribution of 0.9% from MC statistics. When studying the 3π mass distribution, we subtracted the peaking backgrounds using the sideband events. The effect of this approximation has been estimated in the simulation and a specific systematic contribution of 0.7% is estimated. The number of B mesons produced is uncertain to 0.6% [15].

Finally, BABAR measures

$$\mathscr{B}(\mathscr{B}' \to \mathscr{D}^{*-}\pi^+\pi^-\pi^+) = (\iota \in \not\pm \textit{l}.\infty\infty\,(\text{stat.}) \pm \textit{l}.\ni\infty\,(\text{syst.})) \times \infty\textit{l}^{-\ni} \; [16].$$

The result is consistent with the current world average and is 2.4 times more precise. The inclusive branching fraction value without removing the D_s^+ contamination is $(7.37 \pm 0.11 \pm 0.31) \times 10^{-3}$ [16].

References

[1] **BaBar** Collaboration, J.P. Lees et al., *Evidence for an excess of $\bar{B} \to D^{(*)}\tau^-\bar{\nu}_\tau$ decays*, *Phys. Rev. Lett.* **109** (2012) 101802 [`arXiv:1205.5442`].

[2] **Belle** Collaboration, M. Huschle et al., *Measurement of the branching ratio of $\bar{B} \to D^{(*)}\tau^-\bar{\nu}_\tau$ relative to $\bar{B} \to D^{(*)}\ell^-\bar{\nu}_\ell$ decays with hadronic tagging at Belle*, *Phys. Rev.* **D92** (2015) 072014 [`arXiv:1507.03233`].

[3] **Belle** Collaboration, A. Abdesselam et al., *Measurement of the branching ratio of $\bar{B}^0 \to D^{*+}\tau^-\bar{\nu}_\tau$ relative to $\bar{B}^0 \to D^{*+}\ell^-\bar{\nu}_\ell$ decays with a semileptonic tagging method*, `arXiv:1603.06711`.

[4] **LHCb** Collaboration, R. Aaij et al., *Measurement of the ratio of branching fractions* $\mathscr{B}(\bar{B}^0 \to D^{*+}\tau^-\bar{\nu}_\tau)/\mathscr{B}(\bar{B}^0 \to D^{*+}\mu^-\bar{\nu}_\mu)$, *Phys. Rev. Lett.* **115** (2015) 111803 [`arXiv:1506.08614`]. [Addendum: Phys. Rev. Lett.115,no.15,159901(2015)].

[5] S. Fajfer, J.F. Kamenik and I. Nisandzic, *On the $B \to D^*\tau\bar{\nu}_\tau$ Sensitivity to New Physics*, *Phys. Rev.* **D85** (2012) 094025 [`arXiv:1203.2654`].

[6] **Heavy Flavor Averaging Group (HFAG)** Collaboration, Y. Amhis et al., *Averages of b-hadron, c-hadron, and τ-lepton properties as of Summer 2014*, `arXiv:1412.7515`.

[7] D.J. Lange, *The EvtGen particle decay simulation package*, *Nucl. Instrum. Meth.* **A462** (2001) 152.

[8] **GEANT4** Collaboration, S. Agostinelli et al., *GEANT4: A Simulation toolkit*, *Nucl. Instrum. Meth.* **A506** (2003) 250.

[9] **Particle Data Group** Collaboration, K.A. Olive et al., *Review of Particle Physics*, *Chin. Phys.* **C38** (2014) 090001.

[10] G.C. Fox and S. Wolfram, *Event Shapes in e+ e- Annihilation*, *Nucl. Phys.* **B149** (1979) 413. [Erratum: Nucl. Phys.B157,543(1979)].

[11] M. Oreglia, *A Study of the Reactions $\psi' \to \gamma\gamma\psi$*. PhD thesis, SLAC, 1980.

[12] J. Gaiser, *Charmonium Spectroscopy From Radiative Decays of the J/ψ and ψ'*. PhD thesis, SLAC, 1982.

[13] T. Skwarnicki, *A study of the radiative CASCADE transitions between the Upsilon-Prime and Upsilon resonances*. PhD thesis, Cracow, INP, 1986.

[14] **ARGUS** Collaboration, H. Albrecht et al., *Search for Hadronic $b \to u$ Decays*, *Phys. Lett.* **B241** (1990) 278.

[15] **BaBar** Collaboration, J.P. Lees et al., *Time-Integrated Luminosity Recorded by the BABAR Detector at the PEP-II e^+e^- Collider*, *Nucl. Instrum. Meth.* **A726** (2013) 203 [`arXiv:1301.2703`].

[16] **BaBar** Collaboration, J.P. Lees et al., *Measurement of the $B^0 \to D^{*-}\pi^+\pi^-\pi^+$ branching fraction*, *Phys. Rev.* **D94** (2016) 091101 [`arXiv:1609.06802`].

PoS(ICHEP2016)572